

High-temperature behavior of supported graphene: Electron-phonon coupling and substrate-induced doping

Søren Ulstrup,¹ Marco Bianchi,¹ Richard Hatch,¹ Dandan Guan,¹ Alessandro Baraldi,^{2,3} Dario Alfè,⁴ Liv Hornekær,¹ and Philip Hofmann¹

¹*Department of Physics and Astronomy, Interdisciplinary Nanoscience Center, Aarhus University, 8000 Aarhus C, Denmark*

²*Physics Department and CENMAT, University of Trieste, 34127 Trieste, Italy*

³*IOM-CNR Laboratorio TASC, Area Science Park, 34149 Trieste, Italy*

⁴*Department of Earth Sciences, Department of Physics and Astronomy, TYC@UCL, and London Centre for Nanotechnology, University College London, Gower Street, London WC1E 6BT, United Kingdom*

(Received 19 March 2012; published 9 October 2012)

The temperature-dependent electronic structure and electron-phonon coupling of weakly doped supported graphene is studied by angle-resolved photoemission spectroscopy and *ab initio* molecular dynamics simulations. The electron-phonon coupling is found to be extremely weak, reaching the lowest value ever reported for any material. However, the temperature-dependent dynamic interaction with the substrate leads to a complex and dramatic change in the carrier density and type in graphene. These changes in the electronic structure are mainly caused by fluctuations in the graphene-substrate distance.

DOI: [10.1103/PhysRevB.86.161402](https://doi.org/10.1103/PhysRevB.86.161402)

PACS number(s): 73.22.Pr, 65.80.Ck, 71.38.-k, 79.60.-i

Graphene's remarkable transport properties have been one reason for the tremendous interest in this material^{1,2} and have been widely studied.³ Transport measurements give direct access to the quantities that are eventually important for applications, such as the temperature-dependent carrier density and mobility. In such experiments, graphene is typically placed on insulating SiO₂ so that the carrier density can be changed by electric field gating. Placing graphene on SiO₂, however, has been shown to severely reduce the carrier mobility, especially above 200 K, i.e., in the temperature range relevant for applications.^{4,5} This can be improved by choosing a flat and uniform insulator as a substrate, such as hexagonal boron nitride,⁶ but the microscopic mechanism of the mobility reduction is not yet well understood. Here we address this issue by using a combination of angle-resolved photoemission spectroscopy (ARPES) and *ab initio* molecular dynamics, techniques that can give detailed information on the system's spectral properties and are thus complementary to transport measurements.

So far, ARPES investigations of the electron-phonon coupling in graphene have been carried out at a constant, low temperature. The determination of the electron-phonon mass enhancement parameter λ then relies on the observed energy dependence of the electronic self-energy near the Fermi energy E_F . For this approach to be applicable, the sample temperature has to be much lower than the relevant temperature for phonon excitations. For the reported results, this is fulfilled with respect to graphene's very high Debye temperature Θ_D ,⁷ but it might not be fulfilled if the Bloch-Grüneisen temperature Θ_{BG} sets the relevant temperature scale.⁸ For strongly doped graphene ($n \approx 10^{13} \text{ cm}^{-2}$), the electron-phonon scattering was found to be of intermediate strength with $\lambda \approx 0.2\text{--}0.3$.⁹⁻¹¹ For weakly doped graphene, λ appears to be much smaller,¹² but the used methodology ceases to be applicable for weak coupling. Here we employ a different approach to study the electron-phonon coupling directly, by measuring the temperature-dependent self-energy for supported graphene. This necessitates that ARPES experiments be carried out

up to high temperatures but it does not require assumptions about the relevant temperature scale for phonon excitations (Θ_D vs Θ_{BG}). In fact, the determination of the relevant temperature scale for phonon excitations is a by-product of the analysis. We find that λ is extremely small such that temperature-induced mobility reductions would not necessarily be expected, even for supported graphene. However, we also find unexpected temperature-induced changes in the electronic structure near the Fermi energy that, in a transport measurement, would entirely dominate the electron-phonon coupling effect.

ARPES experiments were carried out at the SGM-3 beamline of the synchrotron radiation source ASTRID.¹³ Graphene was prepared on Ir(111) using standard methods.¹⁴ It was chosen as a substrate because graphene is only weakly coupled to the surface, the system is stable over a wide range of temperatures, and using a metal surface avoids the complications due to charging and inhomogeneity expected for insulating SiO₂. The temperature measurements were performed with a thermocouple and an infrared pyrometer. Temperature-dependent data were taken such that the sample was heated by a filament mounted behind it. The filament current was pulsed and the data were acquired during the off part of the heating cycle. The total energy and k resolution were 18 meV and 0.01 \AA^{-1} , respectively. The *ab initio* molecular dynamics calculations were performed with the same methodology as in Ref. 7, using the VASP code.¹⁵ Calculations were performed with the Γ point only at $T = 300$ and 1000 K. Density of states were calculated on representative simulation snapshots, using a $16 \times 16 \times 1$ grid of \mathbf{k} points (128 points). The projected density of states (PDOS) on the carbon atoms was obtained by projecting the Bloch orbitals onto spherical harmonics with $l = 1$, inside spheres of radius 0.86 \AA centered on the C atoms. The PDOS is representative of the density of states due to the p orbitals of the carbon atoms. The calculated PDOS was normalized such that it could be fitted to the analytical linear density of states per unit cell of isolated graphene near the Dirac point.

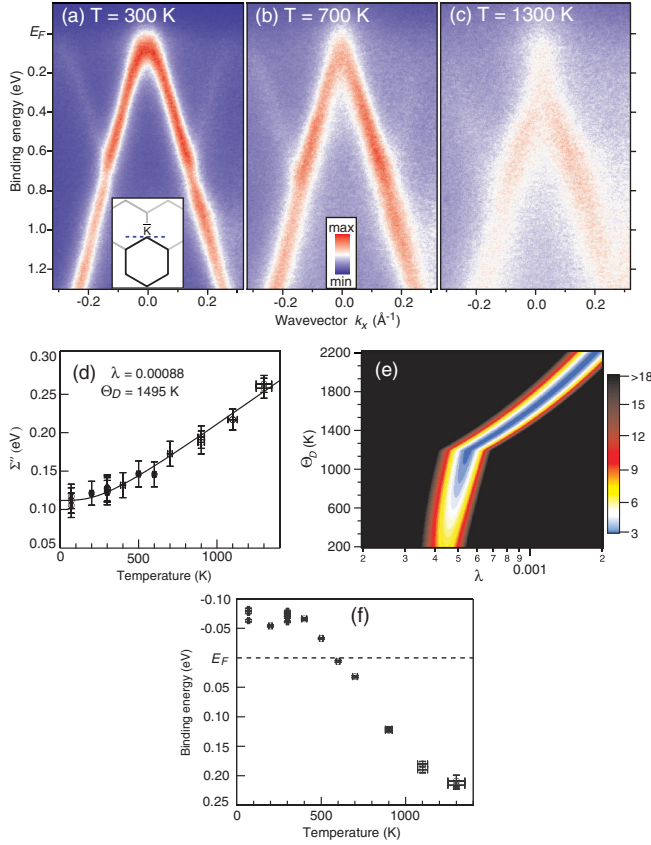


FIG. 1. (Color online) Electronic structure of graphene on Ir(111) determined by ARPES. (a)–(c) Spectra taken through the \bar{K} point of the Brillouin zone perpendicular to the $\bar{\Gamma}$ - \bar{K} direction [dashed line in the inset of (a)] for three different temperatures. k_{\parallel} is measured relative to the Dirac point. (d) Imaginary part of the self-energy below the Dirac point obtained from the MDC linewidth. The solid line is a result of fitting Eq. (1) to the data using the given parameters. (e) χ^2 value for the fit in (d) as a function of the Debye temperature Θ_D and the electron-phonon coupling strength λ . (f) Dirac point energy as a function of temperature, estimated from the extrapolated high binding energy dispersion.

The measured spectral function for graphene supported on Ir(111) is shown in Fig. 1. The electronic structure close to the Fermi energy E_F and near the \bar{K} point of the Brillouin zone is shown for three different temperatures in Figs. 1(a)–1(c). The characteristic Dirac cone is easily identified, even for the highest temperature of 1300 K. In addition to the main Dirac cone, weak replicas and minigaps are evident. These are caused by the interaction with the substrate and the formation of a moiré superstructure.^{16,17} Remarkably, these features are clearly discernible even at the highest temperature. As the temperature is increased, several changes can be observed in the electronic structure. The first is the expected broadening of the features that is caused by the electron-phonon coupling. Given the very large temperature range of the measurements, this effect is relatively minor. The second and unexpected effect is a significant change of the doping. At 300 K the Dirac point of graphene is located above the Fermi energy, in agreement with earlier results,^{16,17} but as the temperature increases, it shifts substantially and is clearly below the Fermi energy at 1300 K.

For a more detailed analysis of the electron-phonon coupling strength, we determine the linewidth of the momentum distribution curves (MDCs) averaged over binding energies from 250 to 550 meV below the Dirac point as a function of temperature. An energy interval was chosen in order to improve the experimental uncertainties. The interval limits were chosen such that the lower limit is always more than a typical phonon energy (≈ 200 meV) away from E_F and neither limit is too close to the Dirac point or the crossing points between the main Dirac cone and the replica bands, as this is known to lead to errors in the linewidth determination.¹⁸

From the average MDC linewidth and the (constant) group velocity v of the band we infer the imaginary part of the self-energy Σ'' (Ref. 19) and plot this as a function of temperature in Fig. 1(d). In the high-temperature limit, such data can directly yield the electron-phonon coupling strength λ because Σ'' is a linear function of T , independent of the phonon spectrum.^{20,21} For a metal, this high-temperature limit is reached for $T \gtrsim \Theta_D$. For graphene, this limit is not reached in our experiments, and it must also be kept in mind that the relevant temperature scale might not be set by Θ_D but rather by Θ_{BG} that could be substantially lower.⁸ We thus have to employ the general expression^{21,22}

$$\Sigma''(T) = \pi \hbar \int_0^{\omega_{\max}} \alpha^2 F(\omega') [1 - f(\omega - \omega') + 2n(\omega') + f(\omega + \omega')] d\omega' + \Sigma''_0, \quad (1)$$

where $\hbar\omega$ is the hole energy, $\hbar\omega'$ is the phonon energy, and $f(\omega)$ and $n(\omega)$ are the Fermi and Bose-Einstein distribution functions, respectively. Σ''_0 is a temperature-independent offset that accounts for electron-electron and electron-defect scattering. The integral extends over all phonon frequencies in the material. $\alpha^2 F(\omega')$ is the Eliashberg coupling function which we approximate by a three-dimensional (3D) Debye model, i.e.,

$$\alpha^2 F(\omega') = \lambda(\omega'/\omega_D)^2 = \lambda(\hbar\omega'/k_B\Theta_D)^2, \quad (2)$$

for $\omega' < \omega_D$ and zero elsewhere.²³ A 3D model is chosen in view of the graphene-substrate interactions, but choosing a two-dimensional (2D) model does not significantly alter the results.

In the further analysis, the data in Fig. 1(d) are fitted using Eqs. (1) and (2). This implies three fit parameters: Σ''_0 , λ , and Θ_D . We could choose to eliminate Θ_D from the fit by using an experimentally determined value [e.g., $\Theta_D = 1495$ K (Ref. 7)]. This, however, ignores the possibility that the actually relevant temperature scale is set by Θ_{BG} rather than the Θ_D . We therefore choose to keep Θ_D in Eq. (2) as a free parameter and emphasize that the resulting Θ_D from the fit is then merely an effective measure of the temperature scale relevant for the electron-phonon scattering. It could be much lower than the actual Debye temperature determined from other experiments. In the fit, Θ_D and λ are strongly correlated through (2).²⁴ Figure 1(e) shows a plot of the resulting quality of the fit (χ^2) as a function of Θ_D and λ and illustrates this correlation. We find equally good fits for a wide range of Θ_D and λ along the minimum of the contour, but only for values of $\Theta_D \gtrsim 1050$ K. For the fit in Fig. 1(d) we use the experimentally determined Θ_D of 1495 K (Ref. 7) and $\lambda = 8.8 \times 10^{-4}$.

We can draw several important conclusions. The first is that λ is very small, between 4×10^{-4} and 2×10^{-3} . To the best of our knowledge, this is the lowest λ value ever determined for any material. The result confirms the theoretical expectation of a vanishing λ near the Dirac point.²⁵ Most earlier ARPES studies have been carried out for significantly stronger doping and have accordingly found higher λ values,^{9–11} but a tendency for a weaker coupling at low doping was also reported.¹² The second conclusion is that the actual Debye temperature of graphene, rather than the Bloch-Grüneisen temperature, appears to be the relevant temperature for the electron-phonon scattering. Again, the uncertainty of Θ_D in the fit is large because of the correlation between Θ_D and λ , but the fit is significantly inferior for Θ_D values below 1050 K. Θ_{BG} , on the other hand, can be estimated to be ≈ 400 K, using the average binding energy of 400 meV below E_D that was used for the extraction of the temperature-dependent linewidth. It is interesting to compare this result to the work of Efetov and Kim, who found that Θ_{BG} sets the relevant temperature scale for transport measurements over a wide range of doping levels.⁸ It is unclear why this is not the case here but we note that there are at least two differences in the electron-phonon coupling as observed in transport and ARPES. The first is that scattering in transport includes a geometrical factor that accounts for the difference in forward and backscattering, something that is irrelevant for the lifetime. The second is that, by the construction of our analysis, optical phonons can contribute to the decay of the photohole in our experiment but they cannot be excited in the transport measurements.

While the electron-phonon coupling is thus consistent with theoretical expectations, the temperature-dependent changes of the electronic structure are highly unexpected. The most dramatic effect is the change from hole doping at low temperature to electron doping at high temperature. Indeed, if we infer the position of the Dirac point from an extrapolation of the occupied bands, its position changes by more than 250 meV over the temperature range explored here [see Fig. 1(f)].

It is tempting to ascribe this behavior to an increased graphene-substrate interaction at higher temperatures. We have investigated this possibility by temperature-dependent *ab initio* molecular dynamics calculations. In these calculations, a layer of graphene is placed on a three layer thick slab of Ir(111) and the atoms of the graphene and two topmost Ir layers are allowed to move for 60 ps, keeping track of the electronic degrees of freedom. Such calculations provide us with the average distance between the carbon atoms and the Ir(111) surface atoms and with the electronic structure of the entire system.

Figure 2(a) gives the calculated density of states (DOS) for the *p* states of a freely suspended graphene layer at 0 K (the *s* states give no significant contribution near the Dirac point energy E_D). It shows the expected features of a zero-gap semiconductor with E_D at the Fermi energy. The electronic structure near E_F is magnified in Fig. 2(b) and plotted together with the expected analytical result for a linear dispersion (solid line). The calculated and analytical results virtually coincide near E_F . Small deviations are only discernible for higher absolute binding energies, as the band structure becomes nonlinear and the van Hove singularities, visible in Fig. 2(a), are approached. Also shown is the calculated DOS at a

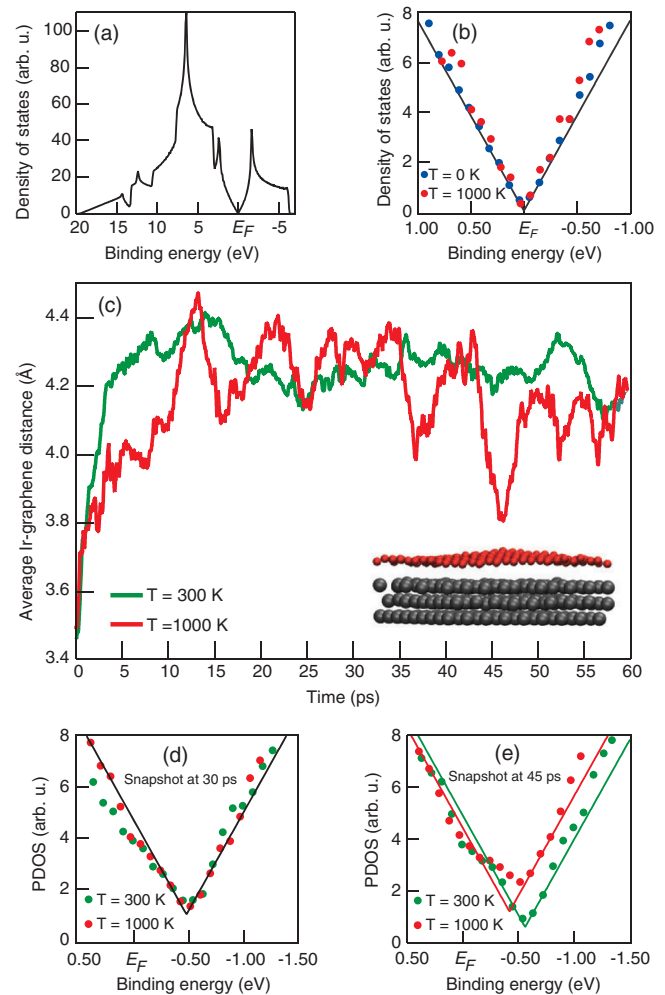


FIG. 2. (Color online) Electronic and geometric structure of suspended and supported graphene determined by *ab initio* molecular dynamics. (a) DOS (from *p* electrons) of freely suspended graphene. (b) DOS for freely suspended graphene in the vicinity of the Fermi energy for two temperatures. The solid line is the DOS calculated from the analytic, linear dispersion. (c) Average distance between the Ir(111) surface and graphene during 60 ps simulations at 300 and 1000 K. The inset shows the geometry of the system after 45 ps at 1000 K. (d) and (e) Snapshots of the projected DOS on the carbon atoms at 30 and 45 ps, corresponding to configurations with similar and different graphene-Ir distances for the two temperatures, respectively. The solid lines have the same shape as in (b) but merely serve as a guide to the eye here.

temperature of 1000 K. Remarkably, the temperature of the graphene has virtually no effect on the DOS. The situation is dramatically different for supported graphene on Ir. Figure 2(c) shows the result of a 60 ps *ab initio* molecular dynamics calculation, giving the average graphene-Ir distance at 300 and 1000 K. After some time needed to achieve thermal equilibrium (around 5 ps), the average distance fluctuates around a stable value. The distance fluctuations are much more pronounced at $T = 1000$ K than at $T = 300$ K. Moreover, the bigger distance fluctuations at 1000 K appear to be periodic, an effect most probably caused by the the long wavelength of the responsible phonons combined with the finite unit cell of the calculation. A smaller average distance between graphene

and the substrate increases their interaction, resulting in a pronounced shift of E_D towards higher binding energies.

This is evident in Figs. 2(d) and 2(e) which show the PDOS on the carbon atoms for two representative configurations: After 30 ps, the graphene-substrate distance is ≈ 4.2 Å for both temperatures and the resulting PDOS curves are nearly identical. After 45 ps, however, the average distance between the graphene layer and the substrate at 1000 K is reduced from ≈ 4.2 to ≈ 3.8 Å and this results in a strong shift of E_D from 560 to 420 meV above E_F , determined by fitting the PDOS with the analytical graphene DOS. What is more, the PDOS is no longer well described by the analytical model, contrary to suspended graphene, with the PDOS at E_D now being substantially different from zero.

The calculations thus reproduce and explain the ARPES observations: Both the pronounced change in doping and the deviation of the spectral function from a simple Dirac cone are caused by fluctuations in the graphene-substrate distance as the temperature is increased. It is tempting to make a more quantitative comparison between experiment and calculations but this would exceed the achievable accuracy in the calculations. The main reason is that the average distance between graphene and the Ir substrate is probably overestimated by the calculations, which do not include the van der Waals interaction. This is the reason for the absolute offset between the doping in experiment and calculation: The artificially large distance gives less wave function overlap and less doping. The experimental trends are, however, well reproduced and we believe the essential physics to be captured. Note that a fluctuating doping of graphene at high temperature would lead to a systematic error in our determination of λ because it represents an additional broadening mechanism. This, however, would merely cause the real λ to be even lower than the value we report above.

The observed temperature-dependent changes of the electronic structure are expected to lead to a very complex behavior in transport measurements, even in the absence of substrate polar phonon modes. In fact, the electron-phonon

coupling would be expected to be insignificant with respect to the other changes that would presumably give rise to a “semiconducting” behavior caused by a strong decrease of the carrier density between 0 and 700 K and a “metallic” behavior above 700 K. Most transport measurements are admittedly limited to a much smaller temperature range, and they would have to be carried out with the graphene placed on an insulator, but our results illustrate that the temperature-dependent doping of supported graphene could have a very significant impact on the transport properties.

In conclusion, we have used spectroscopic measurements showing that the electron-phonon coupling for supported graphene can be extremely weak. Nevertheless, strong effects in the temperature-dependent transport properties can be expected due to temperature-dependent doping changes of the graphene. Our results are also important for a graphene-metal interface in a device where the doping of the graphene under the contacts has important consequences for the operation.²⁶ But they are not restricted to this type of interface. Graphene on SiO₂ is also subject to considerable interface charge transfer²⁷ and similar effects can be expected. Finally, we note that pristine and suspended graphene could be expected to retain its benign electronic properties up to very high temperatures, as our results suggest that the intrinsic electron-phonon coupling is very weak indeed and thermal fluctuations would hardly affect the DOS.

This work was supported by The Danish Council for Independent Research/Technology and Production Sciences and the Lundbeck foundation. A.B. acknowledges the Università degli Studi di Trieste for the *Finanziamento per Ricercatori di Ateneo-FRA2009*. The *ab initio* calculations were performed on the HECToR national service in the UK and the Oak Ridge Leadership Computing Facility, located in the National Center for Computational Sciences at Oak Ridge National Laboratory, which is supported by the Office of Science of the Department of Energy under Contract No. DE-AC05-00OR22725.

¹K. S. Novoselov, A. K. Geim, S. V. Morozov, D. Jiang, Y. Zhang, S. V. Dubonos, I. V. Grigorieva, and A. A. Firsov, *Science* **306**, 666 (2004).

²K. S. Novoselov, A. K. Geim, S. V. Morozov, D. Jiang, M. I. Katsnelson, I. V. Grigorieva, S. V. Dubonos, and A. A. Firsov, *Nature (London)* **438**, 197 (2005).

³S. Das Sarma, S. Adam, E. H. Hwang, and E. Rossi, *Rev. Mod. Phys.* **83**, 407 (2011).

⁴S. V. Morozov, K. S. Novoselov, M. I. Katsnelson, F. Schedin, D. C. Elias, J. A. Jaszczak, and A. K. Geim, *Phys. Rev. Lett.* **100**, 016602 (2008).

⁵J.-H. Chen, C. Jang, S. Xiao, M. Ishigami, and M. S. Fuhrer, *Nat. Nanotechnol.* **3**, 206 (2008).

⁶C. R. Dean, A. F. Young, I. Meric, C. Lee, L. Wang, S. Sorgenfrei, K. Watanabe, T. Taniguchi, P. Kim, K. L. Shepard *et al.*, *Nat. Nanotechnol.* **5**, 722 (2010).

⁷M. Pozzo, D. Alfè, P. Lacovig, P. Hofmann, S. Lizzit, and A. Baraldi, *Phys. Rev. Lett.* **106**, 135501 (2011).

⁸D. K. Efetov and P. Kim, *Phys. Rev. Lett.* **105**, 256805 (2010).

⁹A. Bostwick, T. Ohta, T. Seyller, K. Horn, and E. Rotenberg, *Nat. Phys.* **3**, 36 (2007).

¹⁰A. Bostwick, T. Ohta, J. L. McChesney, T. Seyller, K. Horn, and E. Rotenberg, *Solid State Commun.* **143**, 63 (2007).

¹¹M. Bianchi, E. D. L. Rienks, S. Lizzit, A. Baraldi, R. Balog, L. Hornekær, and P. Hofmann, *Phys. Rev. B* **81**, 041403 (2010).

¹²S. Forti, K. V. Emtsev, C. Coletti, A. A. Zakharov, C. Riedl, and U. Starke, *Phys. Rev. B* **84**, 125449 (2011).

¹³S. V. Hoffmann, C. Søndergaard, C. Schultz, Z. Li, and P. Hofmann, *Nucl. Instrum. Methods Phys. Res., Sect. A* **523**, 441 (2004).

¹⁴J. Coraux, A. T. N'Diaye, M. Engler, C. Busse, D. Wall, N. Buckanie, F.-J. M. zu Heringdorf, R. van Gastel, B. Poelsema, and T. Michely, *New J. Phys.* **11**, 023006 (2009).

¹⁵G. Kresse and J. Furthmüller, *Phys. Rev. B* **54**, 11169 (1996).

¹⁶M. Kralj, I. Pletikosić, M. Petrović, P. Pervan, M. Milun, A. T. N'Diaye, C. Busse, T. Michely, J. Fujii, and I. Vobornik, *Phys. Rev. B* **84**, 075427 (2011).

¹⁷I. Pletikosić, M. Kralj, P. Pervan, R. Brako, J. Coraux, A. T. N'Diaye, C. Busse, and T. Michely, *Phys. Rev. Lett.* **102**, 056808 (2009).

- ¹⁸I. A. Nechaev, M. F. Jensen, E. D. L. Rienks, V. M. Silkin, P. M. Echenique, E. V. Chulkov, and P. Hofmann, *Phys. Rev. B* **80**, 113402 (2009).
- ¹⁹P. Hofmann, I. Y. Sklyadneva, E. D. L. Rienks, and E. V. Chulkov, *New J. Phys.* **11**, 125005 (2009).
- ²⁰B. A. McDougall, T. Balasubramanian, and E. Jensen, *Phys. Rev. B* **51**, R13891 (1995).
- ²¹P. Hofmann and J. W. Wells, *J. Phys.: Condens. Matter* **21**, 013003 (2009).
- ²²G. Grimvall, *The Electron-Phonon Interaction in Metals* (North-Holland, Amsterdam, 1981).
- ²³B. Hellsing, A. Eiguren, and E. V. Chulkov, *J. Phys.: Condens. Matter* **14**, 5959 (2002).
- ²⁴T. K. Kim, T. S. Sorensen, E. Wolfring, H. Li, E. V. Chulkov, and P. Hofmann, *Phys. Rev. B* **72**, 075422 (2005).
- ²⁵M. Calandra and F. Mauri, *Phys. Rev. B* **76**, 205411 (2007).
- ²⁶Y. Wu, V. Perebeinos, Y.-m. Lin, T. Low, F. Xia, and P. Avouris, *Nano Lett.* **12**, 1417 (2012).
- ²⁷H. E. Romero, N. Shen, P. Joshi, H. R. Gutierrez, S. A. Tadigadapa, J. O. Sofo, and P. C. Eklund, *ACS Nano* **2**, 2037 (2008).